

# Kinetics of the Interaction of myo1c with Phosphoinositides\*

Received for publication, July 28, 2009 Published, JBC Papers in Press, August 25, 2009, DOI 10.1074/jbc.M109.049791

Jennine M. Dawicki McKenna<sup>1</sup> and E. Michael Ostap<sup>2</sup>

From the Department of Physiology, Pennsylvania Muscle Institute, University of Pennsylvania School of Medicine, Philadelphia, Pennsylvania 19104-6085

myo1c is a single-headed myosin that dynamically links membranes to the actin cytoskeleton. A putative pleckstrin homology domain has been identified in the myo1c tail that binds phosphoinositides and soluble inositol phosphates with high affinity. However, the kinetics of association and dissociation and the influence of phospholipid composition on the kinetics have not been determined. Stopped-flow spectroscopy was used to measure the binding and dissociation of a recombinant myo1c construct containing the tail and regulatory domains (myo1c<sup>IQ-tail</sup>) to and from 100-nm diameter large unilamellar vesicles (LUVs). We found the time course of association of myo1c<sup>IQ-tail</sup> with LUVs containing 2% phosphatidylinositol 4,5-bisphosphate (PtdIns(4,5)P<sub>2</sub>) followed a two-exponential time course, and the rate of the predominant fast phase depended linearly upon the total lipid concentration. The apparent second-order rate constant was approximately diffusion-limited. Increasing the molar ratio of anionic phospholipid by adding phosphatidylserine, additional PtdIns(4,5)P<sub>2</sub>, or by situating PtdIns(4,5)P<sub>2</sub> in a more physiologically relevant lipid background increased the apparent association rate constant less than 2-fold. myo1c<sup>IQ-tail</sup> dissociated from PtdIns(4,5)P<sub>2</sub> at a slower rate (2.0 s<sup>-1</sup>) than the pleckstrin homology domain of phospholipase C- $\delta$  (13 s<sup>-1</sup>). The presence of additional anionic phospholipid reduced the myo1c<sup>IQ-tail</sup> dissociation rate constant >50-fold but marginally changed the dissociation rate of phospholipase C- $\delta$ , suggesting that additional electrostatic interactions in myo1c<sup>IQ-tail</sup> help to stabilize binding. Remarkably, high concentrations of soluble inositol phosphates induce dissociation of myo1c<sup>IQ-tail</sup> from LUVs, suggesting that phosphoinositides are able to bind to and dissociate from myo1c<sup>IQ-tail</sup> as it remains bound to the membrane.

Myosin-I isoforms are low molecular weight members of the myosin superfamily that link cell membranes with the actin cytoskeleton and play crucial roles driving a diverse array of dynamic membrane processes (1–5). Cell biological studies have shown that myosin-I isoforms localize and fractionate with cell membranes (2, 6), and biochemical experiments have shown myosin-I isoforms bind directly to lipid membranes (7–10). Thus, a key property of some myosin-I isoforms is their ability to bind membranes.

myo1c is a widely expressed vertebrate myosin-I isoform that has roles in a variety of important membrane events, including insulin-stimulated fusion of vesicles containing glucose transporter-4 with the plasma membrane (2, 11), compensatory endocytosis following regulated exocytosis (12), and tensioning of mechano-sensitive ion channels (3). The mechanisms of myo1c targeting and anchoring to specific regions on the membrane to support these functions are not well understood. However, evidence is building that myo1c targeting requires direct binding of myo1c to phosphoinositides in cell membranes (13–16).

We have shown that binding of myo1c to membranes is mediated by a putative pleckstrin homology (PH)<sup>3</sup> domain in its tail that binds phosphatidylinositol 4,5-bisphosphate (PtdIns(4,5)P<sub>2</sub>) and other phosphoinositides with high affinity ( $K_d < 0.5 \mu\text{M}$  in terms of accessible phosphoinositide concentration) (13). myo1c also binds soluble inositol phosphates (e.g. inositol 1,4,5-trisphosphate (InsP<sub>3</sub>)) with similar affinity. Point mutations of amino acids known to be essential for phosphoinositide binding in other PH domains inhibit myo1c binding to PtdIns(4,5)P<sub>2</sub> *in vitro*, and these mutations disrupt membrane localization *in vivo* (13). The affinity of myo1c for PtdIns(4,5)P<sub>2</sub>-containing membranes is increased by the presence of additional anionic phospholipids in the membrane. This increased affinity may be due to nonspecific electrostatic interactions between the anionic phospholipids and positively charged regions within the myo1c tail or regulatory domain (13, 17), which is similar to what has been found for the guanine nucleotide exchange factor, ARNO (18). However, high affinity membrane binding via these nonspecific electrostatic interactions (i.e. binding in the absence of PtdIns(4,5)P<sub>2</sub>) requires the membrane composition to contain a nonphysiological mole fraction (e.g. >40% phosphatidylserine) of anionic phospholipids (13, 14).

Because phosphoinositide binding is important for the cellular localization and function of myo1c (13), it is important to determine the physical constants that define this interaction. Determining the kinetics of membrane attachment will provide insight into the relationship between membrane attachment

\* This work was supported, in whole or in part, by National Institutes of Health Grant GM057247 to (E. M. O.).

<sup>1</sup> Supported by National Institutes of Health Training Grant GM07229 and an American Heart Association predoctoral fellowship.

<sup>2</sup> To whom correspondence should be addressed: B400 Richards Bldg., Philadelphia, PA 19104-6085. E-mail: ostap@mail.med.upenn.edu.

<sup>3</sup> The abbreviations used are: PH, pleckstrin homology; AEDANS-PLC $\delta$ -PH, PLC $\delta$ -PH labeled with IAEDANS; DLS, dynamic light scattering; DOPC, 1,2-dioleoyl-*sn*-glycero-3-phosphocholine; DOPS, 1,2-dioleoyl-*sn*-glycero-3-phospho-L-serine; InsP<sub>3</sub>, inositol 1,4,5-trisphosphate; InsP<sub>6</sub>, phytic acid; LUV, large unilamellar vesicle; PLC $\delta$ , phospholipase-C $\delta$ ; POPC, 1-palmitoyl-2-oleoyl-*sn*-glycero-3-phosphocholine; POPE, 1-palmitoyl-2-oleoyl-*sn*-glycero-3-phosphoethanolamine; POPS, 1-palmitoyl-2-oleoyl-*sn*-glycero-3-phospho-L-serine; PtdIns(3,4,5)P<sub>3</sub>, phosphatidylinositol 3,4,5-trisphosphate; PtdIns(4,5)P<sub>2</sub>, phosphatidylinositol 4,5-bisphosphate; DTT, dithiothreitol; IAEDANS, 5-(((2-iodoacetyl)amino)ethyl)amino)naphthalene-1-sulfonic acid; MES, 4-morpholineethanesulfonic acid.

**TABLE 1**  
Phospholipid composition of LUVs

	Lipid mole fraction				LUV radius <sup>a</sup>	Estimated molecular weight <sup>b</sup>		
	DOPC	DOPS	PtdIns(4,5)P <sub>2</sub>	PtdIns(3,4,5)P <sub>3</sub>				
0.5% PtdIns(4,5)P <sub>2</sub>	0.995	0	0.0050	0	nm	ND		
2% PtdIns(4,5)P <sub>2</sub>	0.980	0	0.0200	0	42 ± 0.60	5.7 × 10 <sup>7</sup>		
8% PtdIns(4,5)P <sub>2</sub>	0.920	0	0.0800	0	48 ± 4.0	8.0 × 10 <sup>7</sup>		
2% PtdIns(4,5)P <sub>2</sub> + 20% DOPS	0.780	0.200	0.0200	0	49 ± 4.7	8.8 × 10 <sup>7</sup>		
2% PtdIns(3,4,5)P <sub>3</sub>	0.980	0	0	0.0200	35 ± 4.1	3.9 × 10 <sup>7</sup>		
	POPE	POPC	POPS	PI	SM	PtdIns(4,5)P <sub>2</sub>	LUV radius <sup>a</sup>	Estimated molecular weight <sup>b</sup>
0.5% PtdIns(4,5)P <sub>2</sub> + lipid mix <sup>d</sup>	0.474	0.199	0.184	0.0920	0.0460	0.0050	ND	ND
2% PtdIns(4,5)P <sub>2</sub> + lipid mix <sup>d</sup>	0.474	0.184	0.184	0.0920	0.0460	0.0200	52 ± 0.55	8.7 × 10 <sup>7</sup>

<sup>a</sup> Values were determined from dynamic light scattering measurements. Errors are S.D. from three to four independent measurements.

<sup>b</sup> Lipid compositions are as defined in Ref. 22.

<sup>c</sup> ND indicates not determined.

<sup>d</sup> Data are from Ref. 24.

and actin attachment lifetimes and will also provide details about the role of anionic lipids in regulating membrane attachment. Therefore, we used stopped-flow kinetics to measure the *in vitro* association and dissociation kinetics of myo1c from LUVs as a function of phosphoinositide composition and anionic charge.

## EXPERIMENTAL PROCEDURES

**Reagents**—InsP<sub>3</sub> was from Calbiochem. Phytic acid (InsP<sub>6</sub>) was from Sigma. The following lipids were from Avanti: 1-palmitoyl-2-oleoyl-*sn*-glycero-3-phosphocholine (POPC), 1-palmitoyl-2-oleoyl-*sn*-glycero-3-phosphoethanolamine (POPE), 1-palmitoyl-2-oleoyl-*sn*-glycero-3-phospho-L-serine (POPS), L- $\alpha$ -phosphatidylinositol (PI), sphingomyelin, L- $\alpha$ -phosphatidylinositol 4,5-bisphosphate (PtdIns(4,5)P<sub>2</sub>), 1,2-dioleoyl-*sn*-glycero-3-phosphocholine (DOPC), 1,2-dioleoyl-*sn*-glycero-3-phospho-L-serine (DOPS), and 1,2-dioleoyl-*sn*-glycero-3-phosphoinositol 3,4,5-trisphosphate (PtdIns(3,4,5)P<sub>3</sub>).

**Protein Expression Constructs**—A construct (myo1c<sup>IQ-tail</sup>) that contains the tail and regulatory domains of mouse myo1c (residues 690–1028) and an N-terminal poly-His tag has been described previously (10). A bacterial construct of the PH domain of phospholipase-C $\delta$  (PLC $\delta$ -PH) was a gift from Dr. M. Lemmon (University of Pennsylvania) and has been described previously (19).

**myo1c Expression and Purification**—myo1c<sup>IQ-tail</sup> was co-expressed with calmodulin in *Sf9* cells using a baculovirus expression system and purified as described previously (10, 14). Briefly, insect cells were co-infected with viruses containing the constructs for myo1c<sup>IQ-tail</sup> and calmodulin. Cells were harvested, lysed in Lysis Buffer (25 mM Tris, pH 7.5, 20 mM imidazole, 300 mM NaCl, 0.5 mM EGTA, 0.5% Igepal, 1 mM  $\beta$ -mercaptoethanol, 1 mM phenylmethylsulfonyl fluoride, 0.01 mg/ml aprotinin, and 0.01 mg/ml leupeptin) and homogenized with a Dounce homogenizer. Lysed cells were centrifuged, and the supernatant, to which DNase and RNase had been added, was sonicated. Lysate was loaded onto a nickel-nitrilotriacetic acid column (Qiagen) and eluted with 125 mM imidazole. myo1c<sup>IQ-tail</sup> was further purified using Mono S and Mono Q FPLC columns (Amersham Biosciences). Purified myo1c<sup>IQ-tail</sup> was dialyzed overnight against HNa100 (10 mM HEPES, pH 7, 100 mM NaCl, 1 mM EGTA, and 1 mM DTT).

**PLC $\delta$ -PH Purification and IAEDANS Labeling**—BL21(DE3)-PLysS cells were transformed with PLC $\delta$ -PH domain plasmid DNA, and protein was expressed and purified as described (20) with slight modifications. Cells were lysed in Lysis Buffer (100 mM NaCl, 10 mM D-glucose, 5 mM DTT, 1 mM phenylmethylsulfonyl fluoride, and 25 mM MES, pH 6). The lysate was sonicated and centrifuged. Supernatant was loaded onto a DEAE-cellulose (Sigma) column, which was pre-equilibrated with Buffer A (50 mM NaCl, 1 mM DTT, and 25 mM MES, pH 6). The column was washed with Buffer A plus 1 mM phenylmethylsulfonyl fluoride. The flow-through, which contained the PLC $\delta$ -PH domain, and wash were then loaded onto an SP-Sepharose Fast Flow column (Sigma) pre-equilibrated with Buffer B (Buffer A without NaCl). The SP column was washed, and protein was eluted in Buffer B with a 0–500 mM NaCl gradient. Protein-containing fractions were ammonium sulfate-precipitated. After centrifugation, the pellet was resuspended in labeling buffer (20 mM Tris, pH 7.5, 150 mM NaCl, 1 mM EGTA) and loaded onto a pre-equilibrated Superdex 200 10/300 GL column (Amersham Biosciences). PLC $\delta$ -PH containing fractions were pooled and labeled with 5-fold molar excess of the thiol-reactive dye, 5-(((2-iodoacetyl)amino)ethyl)amino)naphthalene-1-sulfonic acid (IAEDANS), in labeling buffer at room temperature for 6 h. To remove free dye, labeled protein was passed over a G-25 Fine column pre-equilibrated with HNa100. The efficiency of labeling was 80% as calculated assuming  $\epsilon_{280} = 18,470 \text{ M}^{-1} \text{ cm}^{-1}$  for PLC $\delta$ -PH and  $\epsilon_{336} = 5700 \text{ M}^{-1} \text{ cm}^{-1}$  for IAEDANS.

**Preparation of LUVs**—LUVs were prepared as described previously (14). Briefly, lipids were combined in the molar ratios indicated in Table 1. Solvent was evaporated under a stream of nitrogen. For LUVs composed of complex lipid mixtures, solvent was removed in a rotovap following pre-equilibration at 30 °C to ensure a uniform lipid distribution (21). Dried lipid films were resuspended in HNa100 and briefly vortexed. Lipids underwent five cycles of freeze-thaw before brief bath sonication and 11 passes through 100 nm pore size nitrocellulose membranes (Whatman) in an extruder (Avanti Polar Lipids).

Hydrodynamic radii of LUVs were measured using dynamic light scattering (DLS; Table 1) (Dynamics version 5.26.37).

## Kinetics of the Interaction of myo1c with Phosphoinositides

Radii determined by DLS were used to calculate estimated molecular weights (Table 1) of the LUVs as described (22).

**Stopped-flow Measurements**—All measurements were performed in 10 mM HEPES, pH 7, 100 mM NaCl, 1 mM EGTA, and 1 mM DTT at  $22 \pm 0.1$  °C. Experiments with myo1c<sup>IQ-tail</sup> included 1  $\mu$ M free calmodulin. Association and dissociation transients were acquired using a stopped-flow instrument equipped with removable polarization optics (Applied Photophysics, Spectra Kinetic Work station version 4.54). Light scattering measurements were performed in an L-format with an excitation wavelength of 340 nm and a 320-nm long pass emission filter. A small mixing artifact that was due to light scattering by LUVs was subtracted from transients before fitting. An additional artifact was observed when high concentrations of inositol phosphates (*i.e.* concentrations >1 mM) were mixed with LUVs. Therefore, in InsP<sub>6</sub>-induced dissociation experiments, no more than 1 mM InsP<sub>6</sub> was used, and a blank acquired in the absence of myo1c<sup>IQ-tail</sup> at each InsP<sub>6</sub> concentration was subtracted from transients. Stopped-flow anisotropy measurements were carried out in a T-format with an excitation wavelength of 336 nm and a 475-nm long pass emission filter. Anisotropy was calculated as described (23).

The rate of myo1c<sup>IQ-tail</sup> binding to LUVs at each lipid concentration was determined in each experiment by averaging 2–6 individual traces and fitting to a two-exponential function ( $y = A_{\text{fast}}(1 - e^{-k_{\text{fast}}t}) + A_{\text{slow}}(1 - e^{-k_{\text{slow}}t})$ ). Rates reported for each total lipid concentration were from 1 to 4 experiments. A minimum of five lipid concentrations was assayed for each LUV composition, and the final myo1c<sup>IQ-tail</sup> concentration was 1000-fold below the total lipid concentration. Association transients were acquired under pseudo first-order conditions to obtain apparent second-order rate constants from the slope of a plot of  $k_{\text{fast}}$  versus lipid concentration. Association rate constants are reported as a function of total lipid ( $k_{a\text{-total}}$ ) or LUV concentration ( $k_{a\text{-LUV}}$ ). Reported uncertainties are the standard errors of the fits.

Dissociation rates and amplitudes were obtained by averaging the individual traces from each experiment and fitting to a single exponential function ( $y = A_d(1 - e^{-k_d t})$ ). Average rates and standard deviations from multiple experiments ( $n = 2\text{--}7$ ) are reported (Table 2). For experiments that require large quantities of soluble inositol phosphates (Figs. 1 and 4), myo1c<sup>IQ-tail</sup>-LUV complexes were mixed with InsP<sub>6</sub> to induce dissociation. InsP<sub>6</sub> and InsP<sub>3</sub> bind myo1c<sup>IQ-tail</sup> with similar affinity (13), and InsP<sub>6</sub> is substantially less expensive than InsP<sub>3</sub>.

## RESULTS

**Dissociation of myo1c<sup>IQ-tail</sup> from PtdIns(4,5)P<sub>2</sub>-containing LUVs Is Slowed by the Presence of Additional Anionic Charge**—We measured the rate of dissociation of myo1c<sup>IQ-tail</sup> from PtdIns(4,5)P<sub>2</sub>-containing LUVs by detecting changes in light scattering upon mixing with high concentrations of soluble InsP<sub>3</sub> or InsP<sub>6</sub>, which compete with phosphoinositide-containing LUVs for binding to myo1c<sup>IQ-tail</sup>.

We determined that light scattering linearly reports the concentration of myo1c<sup>IQ-tail</sup> bound to LUVs by showing that the amplitude change upon dissociation is linearly related to protein concentrations between 58 and 460 nM at 115  $\mu$ M total lipid

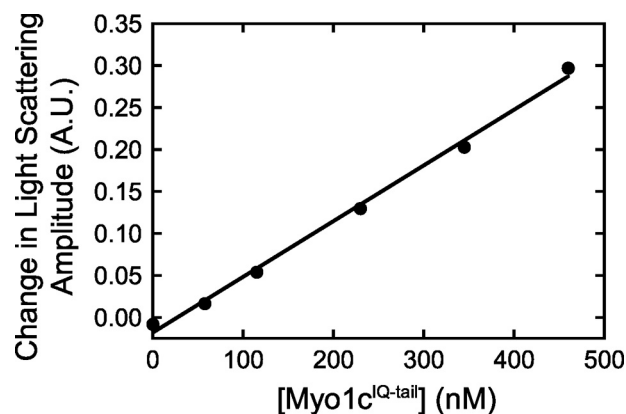


**FIGURE 1. Amplitude change of light scattering of LUVs increases linearly with myo1c<sup>IQ-tail</sup> concentrations.** LUVs containing 2% PtdIns(4,5)P<sub>2</sub> (115  $\mu$ M total lipid) were pre-equilibrated with increasing concentrations of myo1c<sup>IQ-tail</sup> and mixed with either buffer alone or 58  $\mu$ M InsP<sub>6</sub>. Blank-subtracted transients were fit to a single exponential function, and the amplitudes of the fits are plotted as a function of the myo1c<sup>IQ-tail</sup> concentration. The solid line represents a linear fit to the data. Concentrations are after mixing.

concentration (Fig. 1). Transients were difficult to resolve below 58 nM myo1c<sup>IQ-tail</sup> (data not shown). Steady-state binding experiments show that myo1c<sup>IQ-tail</sup> does not bind 100% DOPC LUVs (13, 14), and control stopped-flow experiments showed no significant transient changes in light scattering when inositol phosphates were mixed with 100 nM myo1c<sup>IQ-tail</sup> that was pre-equilibrated with 50  $\mu$ M 100% DOPC LUVs (data not shown).

The time course of 100 nM myo1c<sup>IQ-tail</sup> dissociation from 50  $\mu$ M 2% PtdIns(4,5)P<sub>2</sub> LUVs obtained by mixing with 25  $\mu$ M InsP<sub>3</sub> was best fit with a single exponential function with a rate of  $k_d = 2.0 \pm 0.30$  s<sup>-1</sup> (Fig. 2 and Table 2). The dissociation rate was 8.5-fold faster when the mole percentage of PtdIns(4,5)P<sub>2</sub> was decreased to 0.5% ( $k_d = 17 \pm 0.38$  s<sup>-1</sup>) and was 12-fold slower when the mole percentage of PtdIns(4,5)P<sub>2</sub> was increased to 8% ( $k_d = 0.16 \pm 0.020$  s<sup>-1</sup>; Table 2). The dissociation rate decreased 23-fold ( $k_d = 0.087 \pm 0.020$  s<sup>-1</sup>) when 20% DOPS was included with 2% PtdIns(4,5)P<sub>2</sub> (Fig. 2), and placement of 2% PtdIns(4,5)P<sub>2</sub> in a physiological Lipid Mix (24) that contained POPS, phosphatidylinositol, POPE, POPC, and sphingomyelin (2% PtdIns(4,5)P<sub>2</sub> + Lipid Mix) resulted in an even slower rate of myo1c<sup>IQ-tail</sup> dissociation ( $k_d = 0.025 \pm 0.0030$  s<sup>-1</sup>; Fig. 2). The dramatic decrease in the membrane detachment rate occurs even though myo1c<sup>IQ-tail</sup> does not bind LUVs composed of <40% DOPS (14) or Lipid Mix (data not shown) in the absence of PtdIns(4,5)P<sub>2</sub> with an appreciable affinity. myo1c<sup>IQ-tail</sup> binds LUVs that contain 60% DOPS in the absence of PtdIns(4,5)P<sub>2</sub> (10, 13), but InsP<sub>3</sub> does not induce dissociation from these LUVs (data not shown). Taken together, these results support our model for the presence of two membrane-binding sites within the myo1c<sup>IQ-tail</sup> (13, 14), a phosphoinositide-specific binding site, and a site that binds anionic phospholipids via delocalized electrostatic interactions.

We compared the kinetics of myo1c<sup>IQ-tail</sup> dissociation from 2% PtdIns(4,5)P<sub>2</sub> LUVs with the kinetics of the well characterized phospholipase-C $\delta$  PH domain (19, 25, 26). Dissociation of PLC $\delta$ -PH from 2% PtdIns(4,5)P<sub>2</sub> LUVs did not result in a large enough light scattering change to be detected in our stopped-

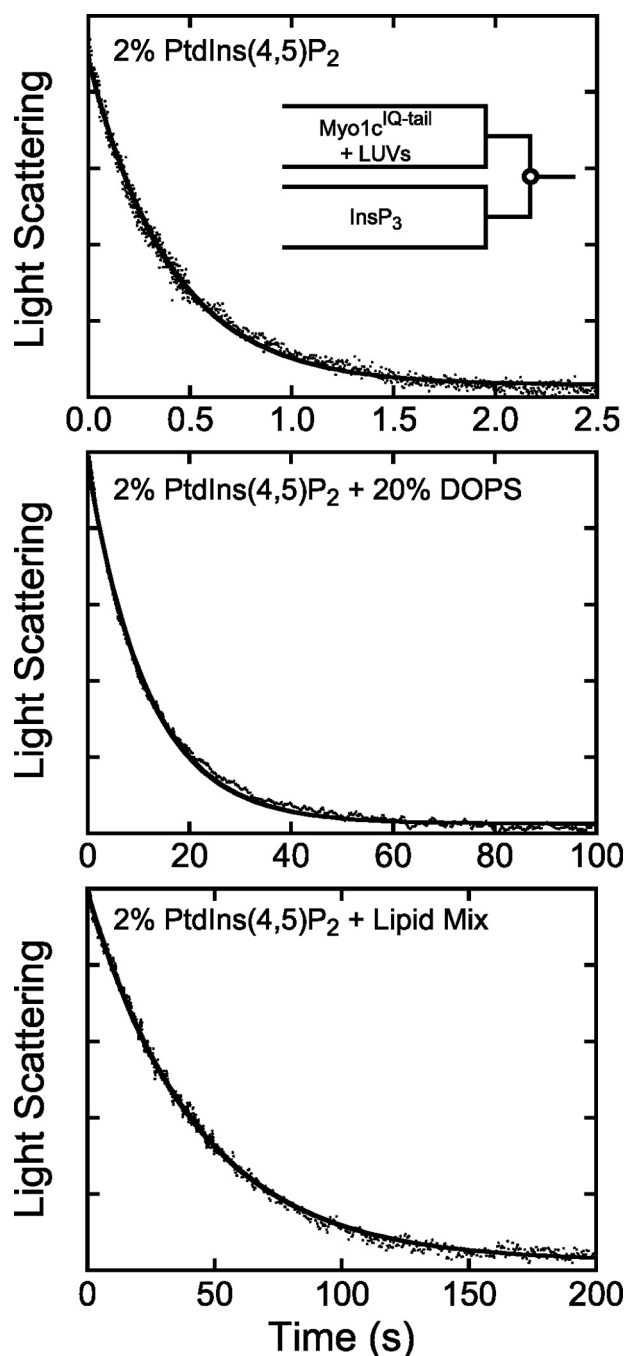


**FIGURE 2. Dissociation of myo1c<sup>IQ-tail</sup> from phosphoinositide-containing LUVs.** Pre-equilibrated solutions of 100 nM myo1c<sup>IQ-tail</sup> and LUVs (50  $\mu$ M total lipid) were rapidly mixed with 25  $\mu$ M InsP<sub>3</sub>, and dissociation was measured as a decrease in light scattering. LUVs were composed of 2% PtdIns(4,5)P<sub>2</sub> (top), 2% PtdIns(4,5)P<sub>2</sub> + 20% DOPS (center), and 2% PtdIns(4,5)P<sub>2</sub> + Lipid Mix (bottom) (Table 1). Experimental time courses (dots) are blank subtracted averages of 2–8 traces. The solid line is the best fit of the data to a single exponential function. Concentrations are after mixing.

flow experiments (data not shown), so we measured changes in fluorescence anisotropy of PLC $\delta$ -PH labeled with IAEDANS (AEDANS-PLC $\delta$ -PH) upon LUV dissociation. Dissociation of AEDANS-PLC $\delta$ -PH from 2% PtdIns(4,5)P<sub>2</sub> LUVs followed a single exponential time course (Fig. 3, top) with a rate ( $13.0 \pm 0.65$  s<sup>-1</sup>) that was faster than measured for myo1c<sup>IQ-tail</sup> (Table 2). Addition of 20% DOPS to 2% PtdIns(4,5)P<sub>2</sub> LUVs decreased

**TABLE 2**  
myo1c<sup>IQ-tail</sup> and PLC $\delta$ -PH dissociation rate constants

The solution used was 10 mM HEPES, pH 7.0, 100 mM NaCl, 1 mM EGTA, 1 mM DTT at  $22 \pm 0.10$  °C. Experiments with myo1c<sup>IQ-tail</sup> included 1  $\mu$ M calmodulin, and dissociation time courses were initiated by mixing with 25  $\mu$ M InsP<sub>3</sub> (100  $\mu$ M InsP<sub>3</sub> for 8% PtdIns(4,5)P<sub>2</sub> LUVs). Errors are the standard deviations. The numbers in parentheses indicate the number of averaged experiments.

LUV composition	myo1c <sup>IQ-tail</sup> $k_d$ s <sup>-1</sup>	AEDANS-PLC $\delta$ -PH $k_d$ s <sup>-1</sup>
2% PtdIns(4,5)P <sub>2</sub>	$2.0 \pm 0.3$ (7)	$13 \pm 0.65$ (3)
2% PtdIns(4,5)P <sub>2</sub> + 1 mM Mg <sup>2+</sup>	$5.8 \pm 0.1$ (2)	
8% PtdIns(4,5)P <sub>2</sub>	$0.16 \pm 0.020$ (3)	
2% PtdIns(4,5)P <sub>2</sub> + 20% DOPS	$0.087 \pm 0.020$ (4)	$6.2 \pm 0.070$ (2)
2% PtdIns(3,4,5)P <sub>3</sub>	$2.8 \pm 1.0$ (6)	
2% PtdIns(3,4,5)P <sub>3</sub> + 1 mM Mg <sup>2+</sup>	$9.1 \pm 5.1$ (3)	
2% PtdIns(4,5)P <sub>2</sub> + Lipid Mix	$0.025 \pm 0.0030$ (3)	$8.3 \pm 0.72$ (2)

the dissociation rate 2-fold ( $6.2 \pm 0.070$  s<sup>-1</sup>), and placement of 2% PtdIns(4,5)P<sub>2</sub> in a physiological Lipid Mix slowed dissociation only 1.5-fold ( $8.3 \pm 0.72$  s<sup>-1</sup>; Fig. 3 and Table 2). Thus, the effect of additional anionic charge on the AEDANS-PLC $\delta$ -PH dissociation rate was substantially smaller than observed for myo1c<sup>IQ-tail</sup>, which is consistent with a single phosphoinositide-specific binding site (26).

**Soluble Inositol Phosphates Induce myo1c<sup>IQ-tail</sup> Dissociation from PtdIns(4,5)P<sub>2</sub>-Containing LUVs**—We examined the time courses of myo1c<sup>IQ-tail</sup>-LUV dissociation as a function of the soluble inositol phosphate concentration. Amplitudes of the dissociation transients show that  $>6.3$   $\mu$ M InsP<sub>6</sub> completely displaces 100 nM myo1c<sup>IQ-tail</sup> from 50  $\mu$ M 2% PtdIns(4,5)P<sub>2</sub> LUVs (Fig. 4, top), as predicted by steady-state competition measurements (13). Surprisingly, the dissociation rates increase hyperbolically with increasing InsP<sub>6</sub> concentrations (Fig. 4), which, under these experimental conditions, is not consistent with a simple competitive binding mechanism as shown in Scheme 1, where,  $k_d$  is a rate-limiting dissociation step. Experiments performed with 6.3–25  $\mu$ M InsP<sub>3</sub> have the same dissociation time courses as those acquired with InsP<sub>6</sub> (data not shown). Additionally, control experiments indicate that the inositol phosphate-induced rate increases are not the result of increases in ionic strength caused by the addition of InsP<sub>3</sub> or InsP<sub>6</sub> (data not shown).

The hyperbolic increase in the dissociation rate suggests a two-step dissociation reaction, which may result from the two membrane-binding sites in the myo1c<sup>IQ-tail</sup>. Therefore, we acquired dissociation transients at a high myo1c<sup>IQ-tail</sup> to accessible PtdIns(4,5)P<sub>2</sub> ratio (5:1) to minimize the number of phosphoinositides bound to myo1c<sup>IQ-tail</sup> via nonspecific electrostatic interactions (Fig. 4, top). The amplitudes of the dissociation transients indicate that InsP<sub>6</sub> completely displaces 0.63  $\mu$ M myo1c<sup>IQ-tail</sup> from 50  $\mu$ M 0.5% PtdIns(4,5)P<sub>2</sub> LUVs. The rates increase hyperbolically with the InsP<sub>6</sub> concentration substantially faster than measured in experiments using 2% PtdIns(4,5)P<sub>2</sub> LUVs (Fig. 4, top).

The dissociation reaction was modeled as shown in Scheme 2, where  $K_1$  is the equilibrium constant for the binding of InsP<sub>6</sub> to LUV-bound myo1c<sup>IQ-tail</sup>;  $k_2$  is the rate of the InsP<sub>6</sub>-induced dissociation step;  $k_3$  is rapid InsP<sub>6</sub> binding to myo1c<sup>IQ-tail</sup>; and  $k_d$  is the rate of InsP<sub>6</sub>-independent dissociation. Assuming  $K_1$  is a rapid equilibrium step and  $k_2$ ,  $k_3$ , and  $k_d$  are effectively irreversible in the presence of high concentrations of InsP<sub>6</sub>, we fit the observed rates to that shown in Equation 1,

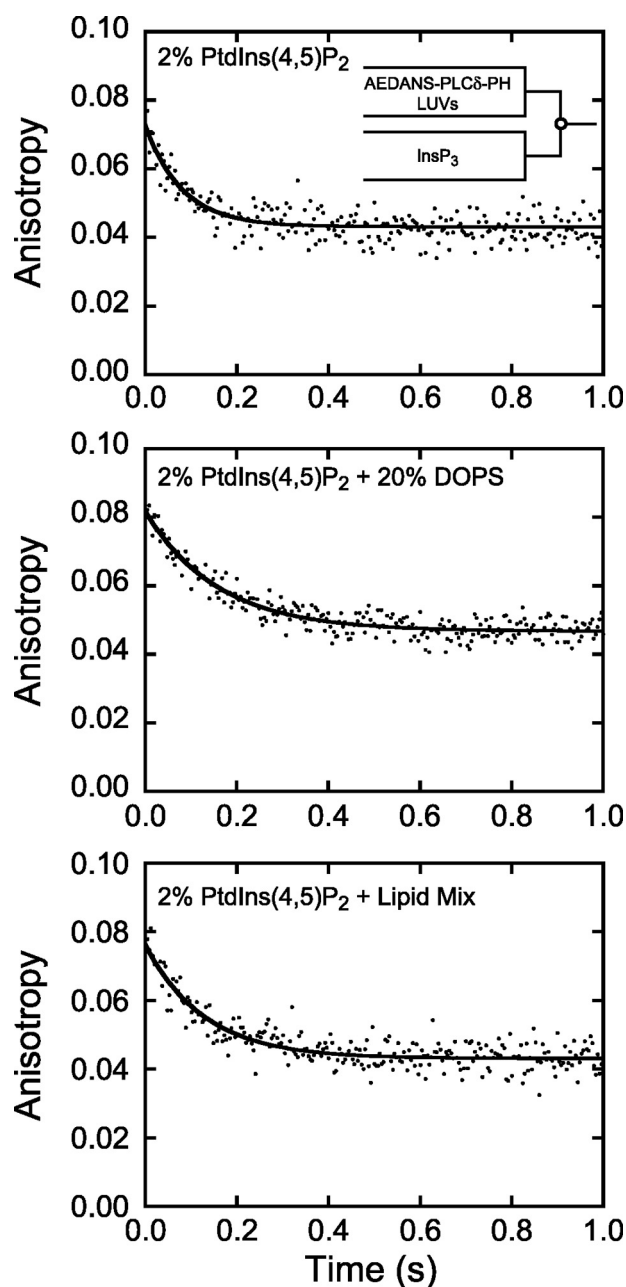


FIGURE 3. **Dissociation of AEDANS-PLC $\delta$ -PH from LUVs.** AEDANS-PLC $\delta$ -PH (5  $\mu$ M) pre-equilibrated with LUVs (1 mM total lipid) was rapidly mixed with 250  $\mu$ M InsP $_3$ , and dissociation was measured as a decrease in fluorescence anisotropy. LUVs were composed of 2% PtdIns(4,5)P $_2$  (top), 2% PtdIns(4,5)P $_2$  + 20% DOPS (center), and 2% PtdIns(4,5)P $_2$  + Lipid Mix (bottom). Experimental time courses (dots) are the average of 2–3 individual traces. Solid lines are fits to a single exponential function. Concentrations are after mixing.

$$k_{\text{obs}} = \frac{k_2[\text{InsP}_6]}{\frac{1}{K_1} + [\text{InsP}_6]} + k_d \quad (\text{Eq. 1})$$

where  $k_d$  is given by the  $y$  intercept. The  $K_1$  values obtained by fitting the 2% PtdIns(4,5)P $_2$  dissociation data ( $K_1 = 420 \pm 120 \text{ M}^{-1}$ ) are 4-fold smaller than found for 0.5% PtdIns(4,5)P $_2$  ( $K_1 = 1600 \pm 170 \text{ M}^{-1}$ ), indicating that higher mole fractions of PtdIns(4,5)P $_2$  make InsP $_6$  binding less favorable (Table 3). The  $k_2$  values from 2% PtdIns(4,5)P $_2$  ( $k_2 = 79 \pm 26 \text{ s}^{-1}$ ) and 0.5%

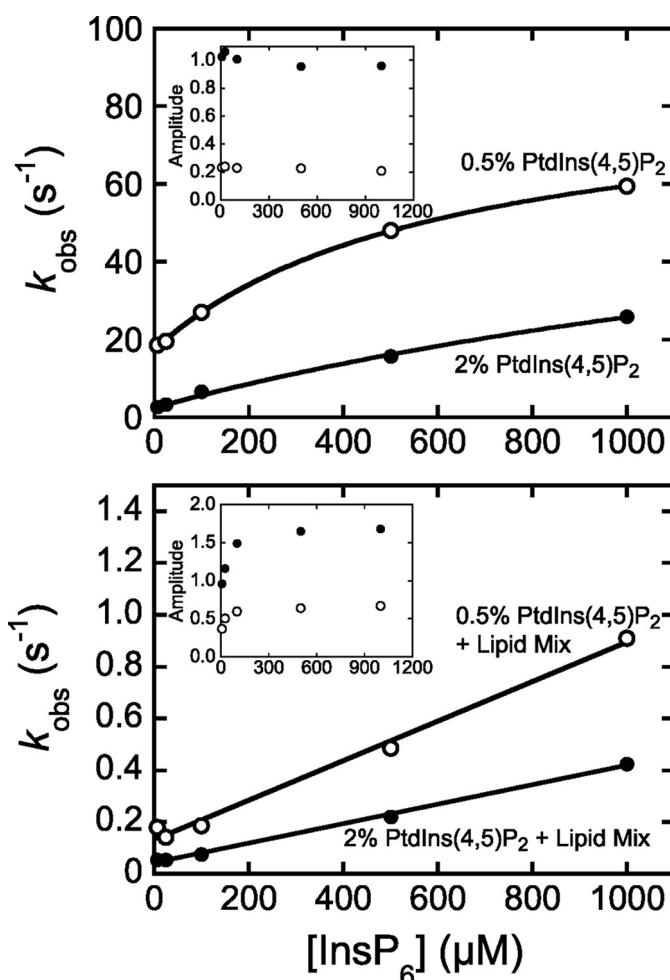
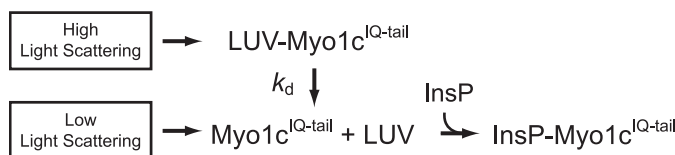


FIGURE 4. **InsP $_6$ -induced dissociation of myo1c<sup>IQ-tail</sup> from phosphoinositide-containing LUVs.** Pre-equilibrated solutions of myo1c<sup>IQ-tail</sup> and LUVs (50  $\mu$ M total lipid) were rapidly mixed with 6.3–1000  $\mu$ M InsP $_6$ , and dissociation was measured as a decrease in light scattering. myo1c<sup>IQ-tail</sup> concentration was 100 nM for 2% PtdIns(4,5)P $_2$  LUVs and 625 nM for all other LUVs. Points are the observed rates, and insets are amplitudes of the transients obtained by fitting to a single exponential function. LUVs were composed of 0.5% PtdIns(4,5)P $_2$  (open symbols) or 2% PtdIns(4,5)P $_2$  (closed symbols) in the absence (top) or presence (bottom) of Lipid Mix (Table 1). Each data point represents the average of 1–2 experiments (each the average of 3–5 transients). The solid lines are the best fits of the data to Equation 1 (top) or a straight line (bottom) with parameters reported in Table 4. Concentrations are after mixing.



SCHEME 1

PtdIns(4,5)P $_2$  ( $k_2 = 68 \pm 2.9 \text{ s}^{-1}$ ), indicate that dissociation occurs rapidly upon InsP $_6$  binding (Table 3). The apparent second-order rate constant for InsP $_6$ -induced dissociation is given by  $K_1k_2$  and is  $1.1 \times 10^5 \text{ M}^{-1}\text{s}^{-1}$  for 0.5% PtdIns(4,5)P $_2$  and  $3.3 \times 10^4 \text{ M}^{-1}\text{s}^{-1}$  for 2% PtdIns(4,5)P $_2$ . The InsP $_6$ -independent dissociation rates from 2% PtdIns(4,5)P $_2$  ( $k_d = 2.8 \pm 0.46 \text{ s}^{-1}$ ) and 0.5% PtdIns(4,5)P $_2$  ( $k_d = 17 \pm 0.40 \text{ s}^{-1}$ ) are consistent with the steady-state LUV affinities and association rate constants (see below).

We also measured the  $\text{InsP}_6$  dependence of  $\text{myo1c}^{\text{IQ-tail}}$  dissociation from LUVs that contained 0.5 and 2%  $\text{PtdIns}(4,5)\text{P}_2$  in a physiological Lipid Mix (Fig. 4, *bottom*). Slightly higher concentrations of  $\text{InsP}_6$  were required to fully dissociate  $\text{myo1c}^{\text{IQ-tail}}$  from the 2%  $\text{PtdIns}(4,5)\text{P}_2$  + Lipid Mix LUVs (Fig. 4, *bottom*), which is consistent with the higher affinity of  $\text{myo1c}^{\text{IQ-tail}}$  for LUVs that contain additional anionic phospholipids (13).  $\text{myo1c}^{\text{IQ-tail}}$  did not bind to LUVs + Lipid Mix when  $\text{PtdIns}(4,5)\text{P}_2$  was

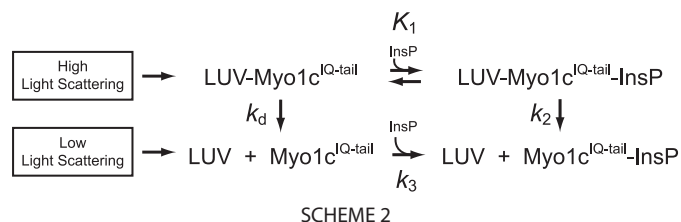


**TABLE 3**  
 $\text{InsP}_6$ -induced-dissociation rate and equilibrium constants

The mixture used was 10 mM HEPES, pH 7.0, 100 mM NaCl, 1 mM EGTA, 1 mM DTT, 1  $\mu\text{M}$  calmodulin at  $22 \pm 0.10^\circ\text{C}$ . Errors are the standard errors of the fits.

LUV composition	$K_1$ $\text{M}^{-1}$	$k_2$ $\text{s}^{-1}$	$k_d$ $\text{s}^{-1}$
0.5% $\text{PtdIns}(4,5)\text{P}_2$	$1600 \pm 170$	$68 \pm 2.9$	$17 \pm 0.40$
2% $\text{PtdIns}(4,5)\text{P}_2$	$420 \pm 120$	$79 \pm 26$	$2.8 \pm 0.46$
	$K_1 k_2$ $\text{M}^{-1} \text{s}^{-1}$		
0.5% $\text{PtdIns}(4,5)\text{P}_2$ + Lipid Mix <sup>a</sup>	$7.6 \times 10^2$		0.13
2% $\text{PtdIns}(4,5)\text{P}_2$ + Lipid Mix <sup>b</sup>	$3.8 \times 10^2$		0.044

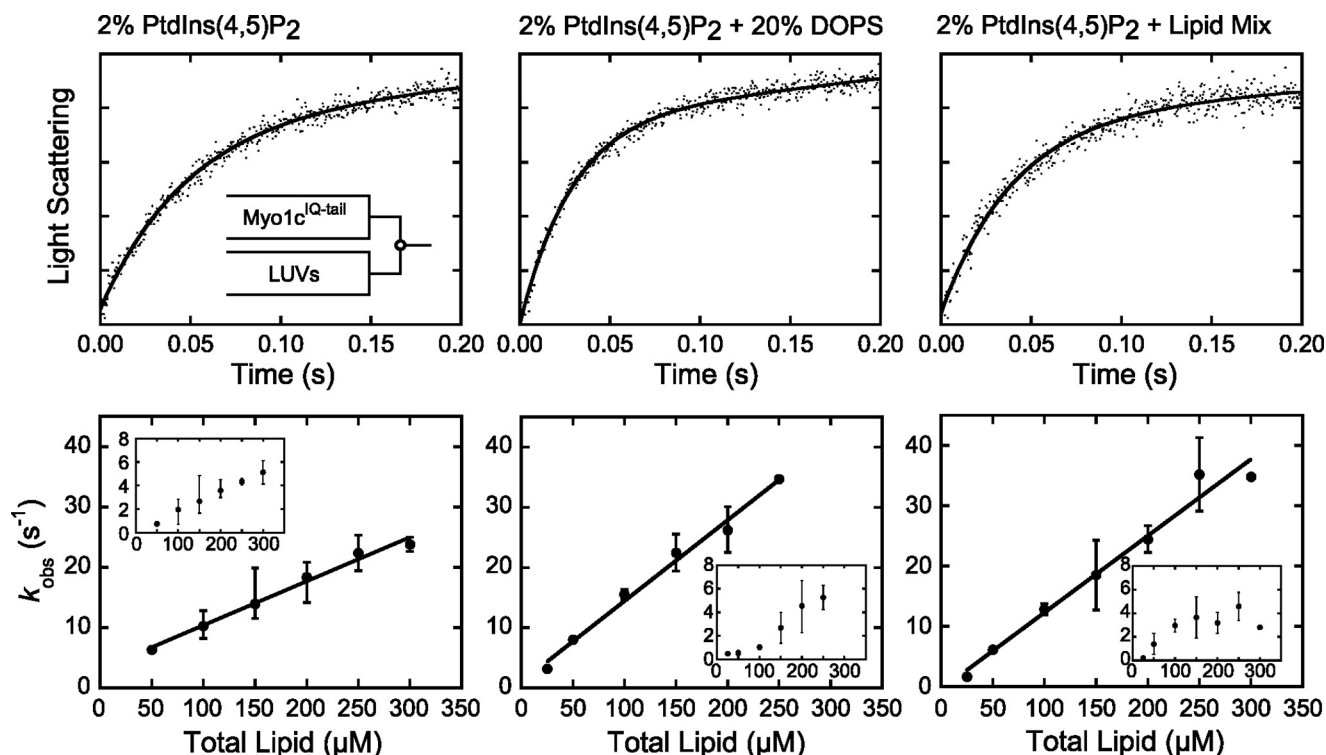
<sup>a</sup> Correlation coefficient for the linear fit equals 0.996.

<sup>b</sup> Correlation coefficient for the linear fit equals 0.999.

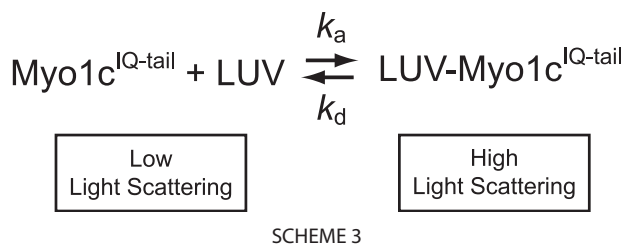
omitted (data not shown). Dissociation rates increased linearly with the  $\text{InsP}_6$  concentration with no sign of a plateau, so we were not able to fit the data to Equation 1. Rather, linear fits to the data give apparent second-order rate constants for  $\text{InsP}_6$ -induced dissociation for 2%  $\text{PtdIns}(4,5)\text{P}_2$  + Lipid Mix ( $K_1 k_2 = 3.8 \times 10^2 \text{M}^{-1} \text{s}^{-1}$ ) and 0.5%  $\text{PtdIns}(4,5)\text{P}_2$  + Lipid Mix ( $K_1 k_2 = 7.6 \times 10^2 \text{M}^{-1} \text{s}^{-1}$ ). If we assume that  $k_2$  is similar to the value obtained above for 2%  $\text{PtdIns}(4,5)\text{P}_2$  (Table 3), the values for  $K_1$  in the presence of Lipid Mix are  $<1 \text{M}^{-1}$ . The  $\text{InsP}_6$ -independent dissociation rates obtained from the  $y$  intercepts for 2%  $\text{PtdIns}(4,5)\text{P}_2$  + Lipid Mix ( $k_d = 0.044 \text{s}^{-1}$ ), and 0.5%  $\text{PtdIns}(4,5)\text{P}_2$  + Lipid Mix ( $k_d = 0.13 \text{s}^{-1}$ ) values are substantially slower than in the absence of Lipid Mix (Table 3).

*Association of myo1c<sup>IQ-tail</sup> to PtdIns(4,5)P<sub>2</sub>-containing LUVs Is Fast and Relatively Independent of Additional Anionic Charge*—Rapid mixing of  $\text{myo1c}^{\text{IQ-tail}}$  with 2%  $\text{PtdIns}(4,5)\text{P}_2$  LUVs resulted in transient increases in light scattering (Fig. 5, *top left*) that were best fit to a two-exponential function, with the average amplitude of the faster of the two phases making up  $>70\%$  of the total. Transient changes in light scattering were not observed when experiments were performed with 100% DOPC LUVs (data not shown). The rates of the fast phase ( $k_{\text{fast}}$ ) increased linearly with the lipid concentration (50–300  $\mu\text{M}$ ), without evidence for a plateau (Fig. 5). The rates of the slow phase ( $k_{\text{slow}} = 0.8\text{--}5.1 \text{s}^{-1}$ ) were much less sensitive to the lipid concentration (Fig. 5).

The apparent second-order rate constant for  $\text{myo1c}^{\text{IQ-tail}}$  binding to LUVs was determined by plotting the rates of the fast

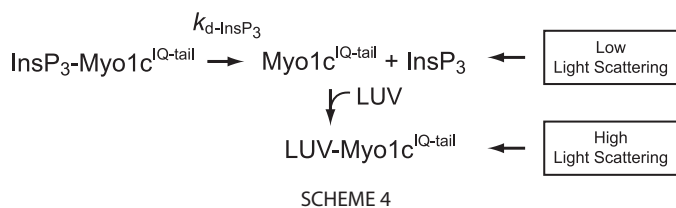


**FIGURE 5. Association of  $\text{myo1c}^{\text{IQ-tail}}$  with LUVs.**  $\text{myo1c}^{\text{IQ-tail}}$  was rapidly mixed with LUVs composed of 2%  $\text{PtdIns}(4,5)\text{P}_2$  (*left*), 2%  $\text{PtdIns}(4,5)\text{P}_2$  + 20% DOPS (*center*), and 2%  $\text{PtdIns}(4,5)\text{P}_2$  + Lipid Mix (*right*). *Top*, experimental time courses of light scattering changes after mixing  $\text{myo1c}^{\text{IQ-tail}}$  with LUVs. Time courses (dots) are blank subtracted averages of traces at final reaction concentrations of 250 nM  $\text{myo1c}^{\text{IQ-tail}}$  and 250  $\mu\text{M}$  total lipids. *Solid lines* are the best fits of the data to a two-exponential function. *Bottom*, rates of  $k_{\text{fast}}$  (closed symbols) and  $k_{\text{slow}}$  (inset) are plotted as a function of total lipid concentration. Each data point represents the average of 1–4 experiments (each the average of 2–6 transients), and the *error bars* report the range of values. The *solid lines* represent linear fits to the data.


**TABLE 4**  
**myo1c<sup>IQ-tail</sup> association rate constants**

 The solution used was 10 mM HEPES, pH 7.0, 100 mM NaCl, 1 mM EGTA, 1 mM DTT, 1  $\mu\text{M}$  calmodulin at  $22 \pm 0.10$  °C. Errors are standard errors of the fits.

LUV composition	$k_{a\text{-total}}$ $\times 10^4 \text{ M}^{-1} \text{ s}^{-1}$	$k_{a\text{-LUV}}$ $\times 10^9 \text{ M}^{-1} \text{ s}^{-1}$	y intercept $\text{s}^{-1}$
2% PtdIns(4,5)P <sub>2</sub>	$7.3 \pm 0.90$	$5.2 \pm 0.70$	$3.0 \pm 1.7$
2% PtdIns(4,5)P <sub>2</sub> + 1 mM Mg <sup>2+</sup>	$3.0 \pm 1.1$	$2.2 \pm 0.90$	$6.9 \pm 2.1$
8% PtdIns(4,5)P <sub>2</sub>	$13 \pm 2.2$	$13 \pm 2.1$	$-0.65 \pm 4.2$
2% PtdIns(4,5)P <sub>2</sub> + 20% DOPS	$13 \pm 0.90$	$14 \pm 1.0$	$1.5 \pm 1.5$
2% PtdIns(3,4,5)P <sub>3</sub>	$10 \pm 1.0$	$4.9 \pm 0.50$	$2.03 \pm 1.73$
2% PtdIns(3,4,5)P <sub>3</sub> + 1 mM Mg <sup>2+</sup>	$7.0 \pm 1.3$	$3.5 \pm 0.60$	$4.0 \pm 2.8$
2% PtdIns(4,5)P <sub>2</sub> + Lipid Mix	$13 \pm 1.5$	$15 \pm 1.7$	$-0.64 \pm 2.58$



phase ( $k_{\text{fast}}$ ) as a function of total lipid concentration (Fig. 5) by assuming the mechanism in Scheme 3, where  $k_a$  and  $k_d$  are the association and dissociation rate constants, respectively.

A linear fit to the data (Fig. 5, *bottom left*) yields an association rate constant  $k_{a\text{-total}} = 7.3 (\pm 0.90) \times 10^4 \text{ M}^{-1} \text{ s}^{-1}$  in terms of total lipid concentration and  $k_{a\text{-LUV}} = 5.2 (\pm 0.70) \times 10^9 \text{ M}^{-1} \text{ s}^{-1}$  in terms of total LUV concentration. The calculated  $k_d$ , given by the y intercept ( $3.0 \pm 1.7 \text{ s}^{-1}$ ; Table 4), is consistent with the InsP<sub>6</sub>-independent dissociation rate measured above (Table 3). Increasing the mole percentage of PtdIns(4,5)P<sub>2</sub> from 2 to 8%, adding 20% PS, or placing 2% PtdIns(4,5)P<sub>2</sub> in a physiological Lipid Mix increased association rate constants less than 2-fold (Fig. 5 and Table 4). Increasing the negative charge in the LUVs also resulted in decreased values of the y intercept, consistent with the dissociation measurements above (Table 4).

**Dissociation of InsP<sub>3</sub> from myo1c<sup>IQ-tail</sup>**—We measured the rate of InsP<sub>3</sub> dissociation from myo1c<sup>IQ-tail</sup> by rapidly mixing 2% PtdIns(4,5)P<sub>2</sub> LUVs (0.6 mM total lipid) with 0.25  $\mu\text{M}$  myo1c<sup>IQ-tail</sup> preincubated with 0.5  $\mu\text{M}$  InsP<sub>3</sub>. Because InsP<sub>3</sub> and PtdIns(4,5)P<sub>2</sub> compete for a binding site on myo1c<sup>IQ-tail</sup> (13), the rate of myo1c<sup>IQ-tail</sup> binding to 2% PtdIns(4,5)P<sub>2</sub> LUVs should be limited by the rate of InsP<sub>3</sub> dissociation at high LUV concentrations as shown in Scheme 4, where  $k_{d\text{-InsP}_3}$  is the rate constant for dissociation of InsP<sub>3</sub> from myo1c<sup>IQ-tail</sup>.

The very high lipid concentration resulted in variable light scattering artifacts in the early time points, so points below 150 ms were not included in the fits. We resolved a transient increase in light scattering that was best fit to a single exponential function with a rate of  $2.2 \pm 0.029 \text{ s}^{-1}$  (Fig. 6), which is

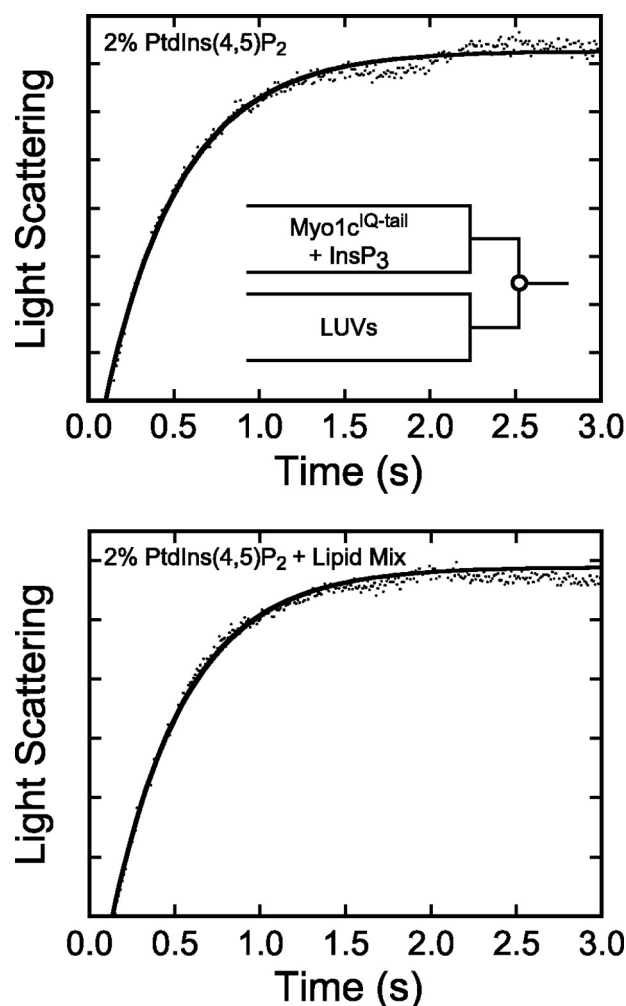


**FIGURE 6. Dissociation of InsP<sub>3</sub> from myo1c<sup>IQ-tail</sup>.** myo1c<sup>IQ-tail</sup> (250 nM) pre-equilibrated with 500 nM InsP<sub>3</sub> was rapidly mixed with LUVs (600  $\mu\text{M}$  total lipid) composed of 2% PtdIns(4,5)P<sub>2</sub> (top), and 2% PtdIns(4,5)P<sub>2</sub> + Lipid Mix (bottom). myo1c<sup>IQ-tail</sup> association with LUVs was measured by light scattering. The first 150 ms of the time courses are not shown because of the presence of a mixing artifact. Experimental time courses (dots) are the average of 3–4 blank-subtracted traces. Solid lines are fits to a single exponential function. Concentrations are after mixing.

20-fold slower than expected for direct binding of myo1c<sup>IQ-tail</sup> to 0.6 mM 2% PtdIns(4,5)P<sub>2</sub> LUVs (Table 4). Rather, we propose that the association rate is limited by  $k_{d\text{-InsP}_3}$  (Scheme 4). A similar rate was also observed when myo1c<sup>IQ-tail</sup> was preincubated with InsP<sub>3</sub> and mixed with LUVs containing 2% PtdIns(4,5)P<sub>2</sub> + Lipid Mix ( $k_{d\text{-InsP}_3} = 2.3 \pm 0.031 \text{ s}^{-1}$ ; see Fig. 6).

**myo1c<sup>IQ-tail</sup> Association and Dissociation Rates Do Not Significantly Differ for 2% PtdIns(4,5)P<sub>2</sub> and 2% PI(3,4,5)P<sub>3</sub> LUVs**—Hokanson *et al.* (13) found that the myo1c<sup>IQ-tail</sup> is able to bind several different soluble inositol phosphates with high affinity. Therefore, we measured the kinetics of the association of myo1c<sup>IQ-tail</sup> with PtdIns(3,4,5)P<sub>3</sub>, as it is an important signaling lipid, and it contains an additional phosphate that could add to the energy of binding. We found the rate of dissociation of myo1c<sup>IQ-tail</sup> from 2% PtdIns(3,4,5)P<sub>3</sub> LUVs ( $k_d = 2.8 \pm 1.0 \text{ s}^{-1}$ ) to be similar to 2% PtdIns(4,5)P<sub>2</sub> LUVs (Table 2). Additionally, myo1c<sup>IQ-tail</sup> associates with 2% PtdIns(3,4,5)P<sub>3</sub> LUVs with a similar association rate constant as to 2% PtdIns(4,5)P<sub>2</sub> LUVs

(Table 4). Therefore, in agreement with steady-state measurements of binding to soluble inositol phosphates (13), the phosphate on the 3-position of the inositol ring does not affect the myo1c<sup>IQ-tail</sup> binding.

Magnesium binds PtdIns(4,5)P<sub>2</sub> in DOPC vesicles (27), and it has been shown to affect the binding of polyphosphoinositide-specific proteins (28). Therefore, we measured myo1c<sup>IQ-tail</sup> dissociation and association in the presence of 1 mM Mg<sup>2+</sup> and found that it slightly increases the rate of myo1c<sup>IQ-tail</sup> dissociation from 2% PtdIns(4,5)P<sub>2</sub> and 2% PtdIns(3,4,5)P<sub>3</sub> LUVs. Magnesium also slightly decreases the rate of association (Table 4).

## DISCUSSION

*Positive Charges in myo1c<sup>IQ-tail</sup> Contribute to Membrane Binding and Slow Dissociation in the Presence of Anionic Lipids*—myo1c<sup>IQ-tail</sup> dissociates from 2% PtdIns(4,5)P<sub>2</sub> LUVs at a rate that is 6.5-fold slower than AEDANS-PLCδ-PH. Additionally, the dissociation rate of myo1c<sup>IQ-tail</sup> decreases up to 80-fold when the mole fraction of anionic phospholipid in the LUVs is increased, which is not the case for AEDANS-PLCδ-PH dissociation (Table 2) or the dissociation of the GRP1 PH domain from PtdIns(3,4,5)P<sub>3</sub> (24). The lipid-dependent kinetic differences between myo1c<sup>IQ-tail</sup> and these other PH domains are likely due to membrane-binding regions outside of the myo1c PH domain. Specifically, previous work has suggested that the positively charged myo1c regulatory domain binds to anionic phospholipids as a secondary membrane attachment site (13, 16, 29). The binding affinity of the regulatory domain interaction for anionic phospholipids does not appear to be high enough to drive membrane binding or confer phosphoinositide specificity (13, 14). However, once bound to the membrane via the phosphoinositide-binding site, the secondary membrane-binding site substantially increases the lifetime of membrane attachment (Table 2). It is an intriguing possibility that once myo1c is bound to the membrane, it remains attached via the secondary binding site, allowing PtdIns(4,5)P<sub>2</sub> to dynamically bind and detach from the myo1c PH domain (below).

*Soluble Inositol Phosphates Induce Membrane Dissociation of myo1c<sup>IQ-tail</sup>*—Knowing the steady-state dissociation constant ( $K_d = 23 \mu\text{M}$  (13)) and the association rate constant ( $k_{a\text{-total}} = 7.3 \times 10^4 \text{ M}^{-1} \text{ s}^{-1}$ ; Table 4) for the interaction of myo1c<sup>IQ-tail</sup> with 2% PtdIns(4,5)P<sub>2</sub> LUVs, the dissociation rate can be calculated ( $k_d = 1.7 \text{ s}^{-1}$ ). This rate is consistent with the basal dissociation rates obtained from the  $y$  intercepts in Figs. 4 and 5. Therefore, in the absence of inositol phosphate-induced dissociation, the basal detachment rate from 2% PtdIns(4,5)P<sub>2</sub> LUVs is  $\sim 2 \text{ s}^{-1}$ . The basal detachment rates are highly dependent on the overall charge of the LUVs, with dissociation rates  $>50$ -fold slower in the presence of additional anionic membranes (Tables 2 and 3).

Increasing the InsP<sub>6</sub> concentration hyperbolically increases the dissociation rate of myo1c<sup>IQ-tail</sup> from LUVs above the basal rate in LUVs that contain phosphoinositides. The simplest model that describes both the enhanced dissociation rate and the hyperbolic dependence is given in Scheme 2 and Equation 1. The equilibrium constant,  $K_1$ , describes the accessibility of the

InsP<sub>6</sub>-binding site.  $K_1$  is modeled as a rapid equilibrium step, meaning that  $k_{+1}$  and  $k_{-1}$  are much greater than  $k_2$ . If  $K_1$  was not a rapid equilibrium step, light scattering time courses would follow a two-exponential rate process. Strikingly, increased mole percentages of anionic phospholipid result in decreased values of  $K_1$ , which range from  $1600 \text{ M}^{-1}$  with LUVs that contain 0.5% PtdIns(4,5)P<sub>2</sub> to  $<1 \text{ M}^{-1}$  with LUVs that contain PtdIns(4,5)P<sub>2</sub> plus Lipid Mix. Despite this large range, the key conclusion that phosphoinositides are able to bind and unbind to myo1c<sup>IQ-tail</sup> whereas the protein remains associated with the membrane has important functional implications (see below).

*Association of myo1c<sup>IQ-tail</sup> with Lipid Vesicles Is Fast and Approaches Diffusion-limited Conditions*—The apparent second-order rate constant for membrane association is fast and increases less than 2-fold in the presence of additional anionic phospholipids (Table 4). The rate of binding approaches the diffusion limit when calculated in terms of LUV concentration (Table 4), which is consistent with previous measurements of binding to LUVs composed of only DOPC and DOPS (10). It should be noted that this result is different from kinetic measurements of the binding of the PH domain from GRP1 to PtdIns(3,4,5)P<sub>3</sub>, which has an  $\sim 6$ -fold increase in its association rate upon inclusion of additional anionic phospholipids (24). It was proposed for the PH domain from GRP1 that nonspecific electrostatic interactions between the PH domain and additional anionic phospholipids facilitate the binding of the PH domain to phosphoinositides (24). It is possible that myo1c follows a similar two-step pathway, except that nonspecific electrostatic interactions between the regulatory domain and anionic phospholipids, including phosphoinositides, facilitate binding to the PH domain.

The slow phase of the myo1c<sup>IQ-tail</sup> association transients makes  $<30\%$  of the total amplitude change. The origin of the slow transition is not known, but it is possible that  $k_{\text{slow}}$  reports the rate of a conformational change in the myo1c<sup>IQ-tail</sup>-LUV complex after binding. It is also possible that this slow kinetic phase is the result of restricted access of myo1c<sup>IQ-tail</sup> to LUVs already occupied with protein. Further spectroscopic experiments are required to resolve this issue.

*Magnesium Affects myo1c<sup>IQ-tail</sup> Dissociation and Association Kinetics*—The presence of 1 mM Mg<sup>2+</sup> decreases the association and increases the dissociation rate constants of myo1c<sup>IQ-tail</sup>-LUV interactions (Tables 2 and 4), but it does not do so in a manner that results in increased specificity for either 2% PtdIns(4,5)P<sub>2</sub> or 2% PtdIns(3,4,5)P<sub>3</sub>. It has been shown that Mg<sup>2+</sup> binds weakly to the head group of PtdIns(4,5)P<sub>2</sub> (27). Thus, Mg<sup>2+</sup> likely competes with myo1c<sup>IQ-tail</sup> for LUV binding, resulting in decreased apparent association rate constants (Table 4). The 3-fold increased rates of dissociation are likely due to the binding of Mg<sup>2+</sup> to the phosphoinositides that are not bound to myo1c<sup>IQ-tail</sup>, reducing the electrostatic interaction between these lipids and positive charges outside of the myo1c PH domain. It is unlikely that the effect of Mg<sup>2+</sup> is because of its binding to calmodulin. Although Mg<sup>2+</sup> binds weakly to calmodulin, this binding has little effect on the overall structure of calmodulin (30).



## Kinetics of the Interaction of myo1c with Phosphoinositides

*Relationship of myo1c<sup>IQ-tail</sup> Membrane Binding Kinetics to the Biochemical Properties of the Motor*—When considering the mechanical activity of myo1c when bound to lipid membranes, it is important to consider how the rate of membrane dissociation relates to the actin attachment time during ATPase cycling. Under unloaded conditions, the maximum actin-activated ATPase rate of myo1c is  $\sim 3 \text{ s}^{-1}$  (31), which is similar to the basal rate of dissociation from 2% PtdIns(4,5)P<sub>2</sub> LUVs ( $k_d = 2.0 \pm 0.30 \text{ s}^{-1}$ ). Thus, there is a significant probability that myo1c would dissociate from a membrane of this composition before completing a catalytic cycle. However, the dissociation rate from membranes containing a more physiological Lipid Mix is substantially slower than the catalytic cycle, and myo1c could undergo multiple catalytic cycles before dissociating. It is important to point out that multiple proteins have recently been identified that bind myo1c, including RalA (32), PHR1 (33), NEMO (34), CaBP1 (35), and CIB (35), and these proteins may play a role in increasing the lifetime of the attachment of myo1c to the membrane and may anchor myo1c for force generation.

*Cell Biological Implications of Membrane Binding Kinetics of myo1c<sup>IQ-tail</sup>*—Phosphoinositide binding via the putative PH domain in the tail appears to be crucial for the membrane localization of myo1c in certain epithelial cell lines (13) and may also be important for its localization in other cell types (16). It is not known if phosphoinositide binding has cellular roles distinct from the spatial regulation of myo1c localization. However, an intriguing possibility is that once bound to phosphoinositides, myo1c concentrates these lipids to regions of high actin concentration, similar to the lateral sequestration of PtdIns(4,5)P<sub>2</sub> by the myristoylated alanine-rich C kinase substrate protein (36).

Given the high concentrations of soluble inositol phosphates required to accelerate dissociation (Fig. 4), it is unlikely that soluble inositol phosphate-induced dissociation is a physiologically relevant dissociation mechanism. Rather, this experimental phenomenon suggests that the phosphoinositide-binding site on myo1c<sup>IQ-tail</sup> is transiently unoccupied, whereas the protein is membrane-bound. Therefore, myo1c may remain attached to the membrane via the secondary binding site, whereas phosphoinositides are free to dissociate from its PH domain and interact with and activate other phosphoinositide-binding proteins. Thus, actin-bound myo1c may act as a “pipmodulin” (21, 36, 37), in that it may spatially control the amount of free PtdIns(4,5)P<sub>2</sub> available for phosphoinositide-activated proteins. Given the predicted importance of phosphoinositides in regulating the formation and dynamics of actin-rich structures (38–41), it will be important to further examine the cellular and mechanical consequences of the myo1c-phosphoinositide interaction.

*Acknowledgments*—We thank Dr. Paul Janmey for assistance with DLS measurements and Dr. Mark Lemmon for the PLC $\delta$ -PH domain construct. We are especially grateful to Dr. Serapion Pырpassopoulos for helpful discussions and Tianming Lin for technical assistance.

## REFERENCES

1. Novak, K. D., Peterson, M. D., Reedy, M. C., and Titus, M. A. (1995) *J. Cell Biol.* **131**, 1205–1221
2. Bose, A., Guilherme, A., Robida, S. I., Nicoloso, S. M., Zhou, Q. L., Jiang, Z. Y., Pomerleau, D. P., and Czech, M. P. (2002) *Nature* **420**, 821–824
3. Holt, J. R., Gillespie, S. K., Provance, D. W., Shah, K., Shokat, K. M., Corey, D. P., Mercer, J. A., and Gillespie, P. G. (2002) *Cell* **108**, 371–381
4. Tyska, M. J., and Mooseker, M. S. (2004) *J. Cell Biol.* **165**, 395–405
5. Laakso, J. M., Lewis, J. H., Shuman, H., and Ostap, E. M. (2008) *Science* **321**, 133–136
6. Ruppert, C., Godel, J., Müller, R. T., Kroschewski, R., Reinhard, J., and Bähler, M. (1995) *J. Cell Sci.* **108**, 3775–3786
7. Adams, R. J., and Pollard, T. D. (1989) *Nature* **340**, 565–568
8. Miyata, H., Bowers, B., and Korn, E. D. (1989) *J. Cell Biol.* **109**, 1519–1528
9. Hayden, S. M., Wolenski, J. S., and Mooseker, M. S. (1990) *J. Cell Biol.* **111**, 443–451
10. Tang, N., Lin, T., and Ostap, E. M. (2002) *J. Biol. Chem.* **277**, 42763–42768
11. Bose, A., Robida, S., Furcinitti, P. S., Chawla, A., Fogarty, K., Corvera, S., and Czech, M. P. (2004) *Mol. Cell Biol.* **24**, 5447–5458
12. Sokac, A. M., Schietroma, C., Gundersen, C. B., and Bement, W. M. (2006) *Dev. Cell* **11**, 629–640
13. Hokanson, D. E., Laakso, J. M., Lin, T., Sept, D., and Ostap, E. M. (2006) *Mol. Biol. Cell* **17**, 4856–4865
14. Hokanson, D. E., and Ostap, E. M. (2006) *Proc. Natl. Acad. Sci. U.S.A.* **103**, 3118–3123
15. Huang, S., Lifshitz, L., Patki-Kamath, V., Tuft, R., Fogarty, K., and Czech, M. P. (2004) *Mol. Cell Biol.* **24**, 9102–9123
16. Hirono, M., Denis, C. S., Richardson, G. P., and Gillespie, P. G. (2004) *Neuron* **44**, 309–320
17. Swanlung-Collins, H., and Collins, J. H. (1994) *Adv. Exp. Med. Biol.* **358**, 205–213
18. Macia, E., Paris, S., and Chabre, M. (2000) *Biochemistry* **39**, 5893–5901
19. Lemmon, M. A., Ferguson, K. M., O'Brien, R., Sigler, P. B., and Schlessinger, J. (1995) *Proc. Natl. Acad. Sci. U.S.A.* **92**, 10472–10476
20. Ferguson, K. M., Lemmon, M. A., Schlessinger, J., and Sigler, P. B. (1994) *Cell* **79**, 199–209
21. Gambhir, A., Hangyás-Mihályné, G., Zaitseva, I., Cafiso, D. S., Wang, J., Murray, D., Pentyala, S. N., Smith, S. O., and McLaughlin, S. (2004) *Bioophys. J.* **86**, 2188–2207
22. Lu, Y., and Nelsestuen, G. L. (1996) *Biochemistry* **35**, 8193–8200
23. Lakowicz, J. R. (1999) *Principles of Fluorescence Spectroscopy*, 2nd Ed., Kluwer Academic/Plenum Publishers, New York
24. Corbin, J. A., Dirckx, R. A., and Falke, J. J. (2004) *Biochemistry* **43**, 16161–16173
25. Lemmon, M. A., and Ferguson, K. M. (2001) *Biochem. Soc. Trans.* **29**, 377–384
26. Ferguson, K. M., Lemmon, M. A., Schlessinger, J., and Sigler, P. B. (1995) *Cell* **83**, 1037–1046
27. Toner, M., Vaio, G., McLaughlin, A., and McLaughlin, S. (1988) *Biochemistry* **27**, 7435–7443
28. Dove, S. K., Piper, R. C., McEwen, R. K., Yu, J. W., King, M. C., Hughes, D. C., Thuring, J., Holmes, A. B., Cooke, F. T., Michell, R. H., Parker, P. J., and Lemmon, M. A. (2004) *EMBO J.* **23**, 1922–1933
29. Collins, J. H., and Swanlung-Collins, H. (1992) *Adv. Exp. Med. Biol.* **321**, 159–163
30. Gifford, J. L., Walsh, M. P., and Vogel, H. J. (2007) *Biochem. J.* **405**, 199–221
31. Manceva, S., Lin, T., Pham, H., Lewis, J. H., Goldman, Y. E., and Ostap, E. M. (2007) *Biochemistry* **46**, 11718–11726
32. Chen, X. W., Leto, D., Chiang, S. H., Wang, Q., and Saltiel, A. R. (2007) *Dev. Cell* **13**, 391–404
33. Etournay, R., El-Amraoui, A., Bahloul, A., Blanchard, S., Roux, I., Pézeron, G., Michalski, N., Daviet, L., Hardelin, J. P., Legrain, P., and Petit, C. (2005) *J. Cell Sci.* **118**, 2891–2899
34. Nakamori, Y., Emoto, M., Fukuda, N., Taguchi, A., Okuya, S., Tajiri, M., Miyagishi, M., Taira, K., Wada, Y., and Tanizawa, Y. (2006) *J. Cell Biol.*

- 173, 665–671
35. Tang, N., Lin, T., Yang, J., Foskett, J. K., and Ostap, E. M. (2007) *J. Muscle Res. Cell Motil.* **28**, 285–291
36. McLaughlin, S., and Murray, D. (2005) *Nature* **438**, 605–611
37. Laux, T., Fukami, K., Thelen, M., Golub, T., Frey, D., and Caroni, P. (2000) *J. Cell Biol.* **149**, 1455–1472
38. Kölsch, V., Charest, P. G., and Firtel, R. A. (2008) *J. Cell Sci.* **121**, 551–559
39. Yin, H. L., and Janmey, P. A. (2003) *Annu. Rev. Physiol.* **65**, 761–789
40. Brozinick, J. T., Jr., Berkemeier, B. A., and Elmendorf, J. S. (2007) *Curr. Diabetes Rev.* **3**, 111–122
41. Insall, R. H., and Weiner, O. D. (2001) *Dev. Cell* **1**, 743–747